CHAPTER

# Construction of Odor Representations by Olfactory Bulb Microcircuits

7

**Thomas A. Cleland**[1]

*Department of Psychology, Cornell University, Ithaca, NY, USA*

*[1]Corresponding author: Tel.: +1-607-255-8099; Fax: +1-775-254-2756, e-mail address: tac29@cornell.edu*

## Abstract

Like other sensory systems, the olfactory system transduces specific features of the external environment and must construct an organized sensory representation from these highly fragmented inputs. As with these other systems, this representation is not accurate *per se*, but is constructed for utility, and emphasizes certain, presumably useful, features over others. I here describe the cellular and circuit mechanisms of the peripheral olfactory system that underlie this process of sensory construction, emphasizing the distinct architectures and properties of the two prominent computational layers in the olfactory bulb. Notably, while the olfactory system solves essentially similar conceptual problems to other sensory systems, such as contrast enhancement, activity normalization, and extending dynamic range, its peculiarities often require qualitatively different computational algorithms than are deployed in other sensory modalities. In particular, the olfactory modality is intrinsically high dimensional, and lacks a simple, externally defined basis analogous to wavelength or pitch on which elemental odor stimuli can be quantitatively compared. Accordingly, the quantitative similarities of the receptive fields of different odorant receptors (ORs) vary according to the statistics of the odor environment. To resolve these unusual challenges, the olfactory bulb appears to utilize unique nontopographical computations and intrinsic learning mechanisms to perform the necessary high-dimensional, similarity-dependent computations. In sum, the early olfactory system implements a coordinated set of early sensory transformations directly analogous to those in other sensory systems, but accomplishes these with unique circuit architectures adapted to the properties of the olfactory modality.

## Keywords

olfactory bulb circuitry, odor space, similarity space, perceptual space, odor representations, small-world network, categorization, decorrelation, generalization, nontopographical contrast enhancement, spare receptor capacity, receptor reserve, feedback normalization, gamma oscillations

**Progress in Brain Research, Volume 208, ISSN 0079-6123, http://dx.doi.org/10.1016/B978-0-444-63350-7.00007-3**

## 1 INTRODUCTION

All of the information that an organism possesses about the world—the entire extrinsic knowledge base upon which it bases behavioral decisions—is obtained via its sensory systems. The performance of sensory systems hence is fundamentally limiting, especially given that the physics of the natural world is not optimized for organisms' benefit. Physical signals that are predictive of immediate danger, changing seasons, potential resources, or the presence of conspecifics generally do not stand out as elemental stimuli, but are diagnostic only as statistically unusual combinations of environmental phenomena. The signals generated by important states and events (generically, *situations*) can be—and often are—quite similar to those of unimportant phenomena, requiring a careful parsing of sensory input patterns in order to distinguish potentially important environmental states or events from meaningless background. Moreover, the signals generated by important situations are themselves variable—both at the source and owing to degradation between emission and reception—necessitating a determination of *how much* variance in a detected signal is still likely to be indicative of a important situation. How different from a known important stimulus, and in what ways, does some detected signal need to be in order to be dismissed as not representative of that stimulus or its implications? How does one optimize the signal-detection capacities of a sensory system to maximize the ability to identify important signals while rejecting similar but unimportant signals? This fundamental problem applies across sensory systems—from the basic physicoresponsive and chemoresponsive properties of bacteria (Krell et al., 2010) to the diverse, traditionally recognized "senses" of complex animals: vision, audition, somatosensation (touch), and the multimodal chemical senses including olfaction, taste, and the vomeronasal and trigeminal systems—although the underlying mechanisms and computations can vary substantially. In this chapter, I describe the sensory mechanisms and computations of the vertebrate olfactory system, both in their unique application to the chemosensory modality and with reference to the core principles common among sensory systems.

Across modalities, the sensory process can be conceptually condensed to two sequential stages: *transduction* and *construction*. Transduction in this context refers to the translation of some form of environmental variance into neural activity variance. To successfully transduce any environmental phenomenon into a detectable signal requires an appropriate sensor—some cellular/molecular machine that is capable of making this conversion from light, pressure waves, chemical vapors, or other stimuli into neural activity. The specializations of each such sensory machine determine the range of stimulus qualities that will evoke this neural activity, and this range comprises that cell's *receptive field*. Receptive fields can be relatively broad (respond to a wide range of stimuli) or relatively narrow (responding more selectively), but in all cases, the common theme is that signals of interest within complex natural environmental scenes are detected piecemeal by arrays of dedicated, highly limited physical sensors and subsequently must be *constructed* within the brain into organized sensory representations that enable the animal to utilize the

information. Importantly, the constructed representation need not faithfully replicate the external signal—and in fact rarely does. Rather, certain aspects of external signals typically are overrepresented and others are underrepresented by sensory systems, in accordance with the interests of the organism. For example, some terrestrial visual systems are optimized for a $1/f$ distribution of spatial frequencies, matching the distribution observable within natural visual scenes (Geisler, 2008), and certain ecologically important, species-specific auditory frequency bands are overrepresented in the tonotopic maps of the auditory brainstem (Koppl et al., 1993; Zook and Leake, 1989). What is the olfactory equivalent of this sensory optimization for ethologically relevant components of natural scene statistics? How are transduction and construction mechanisms coordinated to achieve such optimizations?

At the transduction stage, mediated by primary sensory receptors, one important priority is simply to maximize the capacity to gather information about the environment—that is, to deploy receptors that are sensitive to any physical phenomenon that might potentially contribute to signals of interest. Signals that are not transduced are lost. However, all phenomena are not equally meaningful; accordingly, a second, somewhat conflicting priority is to deploy limited sensory resources optimally. This applies to both the transduction and construction stages. In the case of transduction, increasing the number of expressed receptor types with receptive fields tuned for aspects of common, ecologically important signals improves sensitivity and discrimination capacity for these signals, at the cost of reducing sensitivity and discrimination capacity for less common, possibly less ecologically important signals by deploying fewer receptors sensitive to these signals. At the construction stage, this process of selective emphasis can be repeated. Additionally, particular *combinations* of signals incorporating more than one receptor type—and diagnostic of more specific sensory phenomena—can be recognized at these later stages and selectively emphasized. Top-down inputs such as memory, motivation, and information from other modalities also can modify sensory construction, but no additional afferent information will be available other than that which was originally transduced. The construction stage continues indefinitely—there is no clear boundary between sensory construction and higher cognition—but the concept is most readily applied to the relatively peripheral neural circuits that specialize to some degree in parsing clearly sensory information. Importantly, such circuits can have functions ranging from mundane compensation for the limitations of sensory transducers to the rich incorporation of top-down information about prior knowledge and behavioral state. Ultimately, the task is to construct and interpret certain important features of the external scene from the patterns of elemental activation generated by the transduction layer.

## 2 OLFACTORY TRANSDUCTION AND CONVERGENCE

Olfactory transduction occurs in the nasal cavity, where ciliated primary olfactory sensory neurons (OSNs), covered with a layer of mucus, populate a portion of the nasal epithelium. Inhaled odorous molecules dissolve into the mucus layer and

associate with the extracellular binding sites of OR proteins located on OSN cilia (Getchell, 1986; Morrison and Costanzo, 1990, 1992). These associations trigger transduction cascades within the cilia that depolarize the OSN and evoke a train of action potentials, the frequency of which depends systematically on the intensity of the odor-evoked depolarization (Getchell and Shepherd, 1978; Rospars et al., 2000). These spike trains are temporally unsophisticated and are generally considered to be simple rate codes reporting the intensity of activation of the corresponding OSN, though they also are moderately affected by intracellular adaptation processes that serve to emphasize transient changes in the intensity of activation (Zufall and Leinders-Zufall, 2000).

There are roughly 350 different types of ORs expressed in the human nose, and roughly 1000–1200 in mice and rats (Mombaerts, 1999, 2001). Canonically, only one type of OR is expressed in any single OSN. This may not be exhaustively true across all cells and species (Mombaerts, 2004); however, in mice, this exclusion can extend to only one allelic variant of one OR being expressed in individual OSNs (Chess et al., 1994). Groups of OSNs that express the same OR (referred to as *sister OSNs*, or OSN classes) consequently are activated by the same odor ligands. OSNs project axons across the blood–brain barrier into the olfactory bulb (Fig. 1)—the first central nervous system structure of the olfactory system. Critically, the axons of sister OSNs converge together (Mombaerts et al., 1996), such that their axonal arbors intertwine into tangles of neuropil from thousands of OSNs expressing the same OR, and excluding the axonal arbors of OSNs expressing different ORs, within the surface layer of the olfactory bulb. These discrete tangles of neuropil are visible at the light microscopic level as spheroid structures of roughly 40–100 μm diameter and termed *glomeruli* (singular: glomerulus). As each glomerulus comprises the axonal arborizations of OSNs expressing the same OR, the number of glomeruli directly reflects the number of different ORs expressed by a given species. In mice, for example, there are more than 1000 different ORs, and approximately twice that many glomeruli in each olfactory bulb, because most glomeruli are duplicated in the medial and lateral olfactory bulb (Schoenfeld and Cleland, 2005).

As the olfactory epithelium contains millions of OSNs, there are on the order of thousands of sister OSNs expressing each type of OR. As different ORs are responsive to different chemical epitopes of odorous molecules, any given odorant—whether comprising a single type of molecule or a consistent ratio of many different odorous molecules—typically will activate a consistent set of several different classes of OSN. Moreover, each OSN class will be activated to a different extent depending on the potency of the odor ligand for each OR type, such that the resulting pattern of relative activation levels among multiple OSN classes (a "relational representation"; Cleland et al., 2007) contains information about the odor ligands that are present. However, odorant concentrations also strongly affect OSN activation levels, and this constitutes a major problem for odor identification. Simple ligand–receptor binding curves are constrained by statistical mechanics to go from mostly dissociated (e.g., 10% bound) to near-maximally associated (e.g., 90% bound) within a narrow ligand concentration range, less than two orders of magnitude. Indeed, concentration

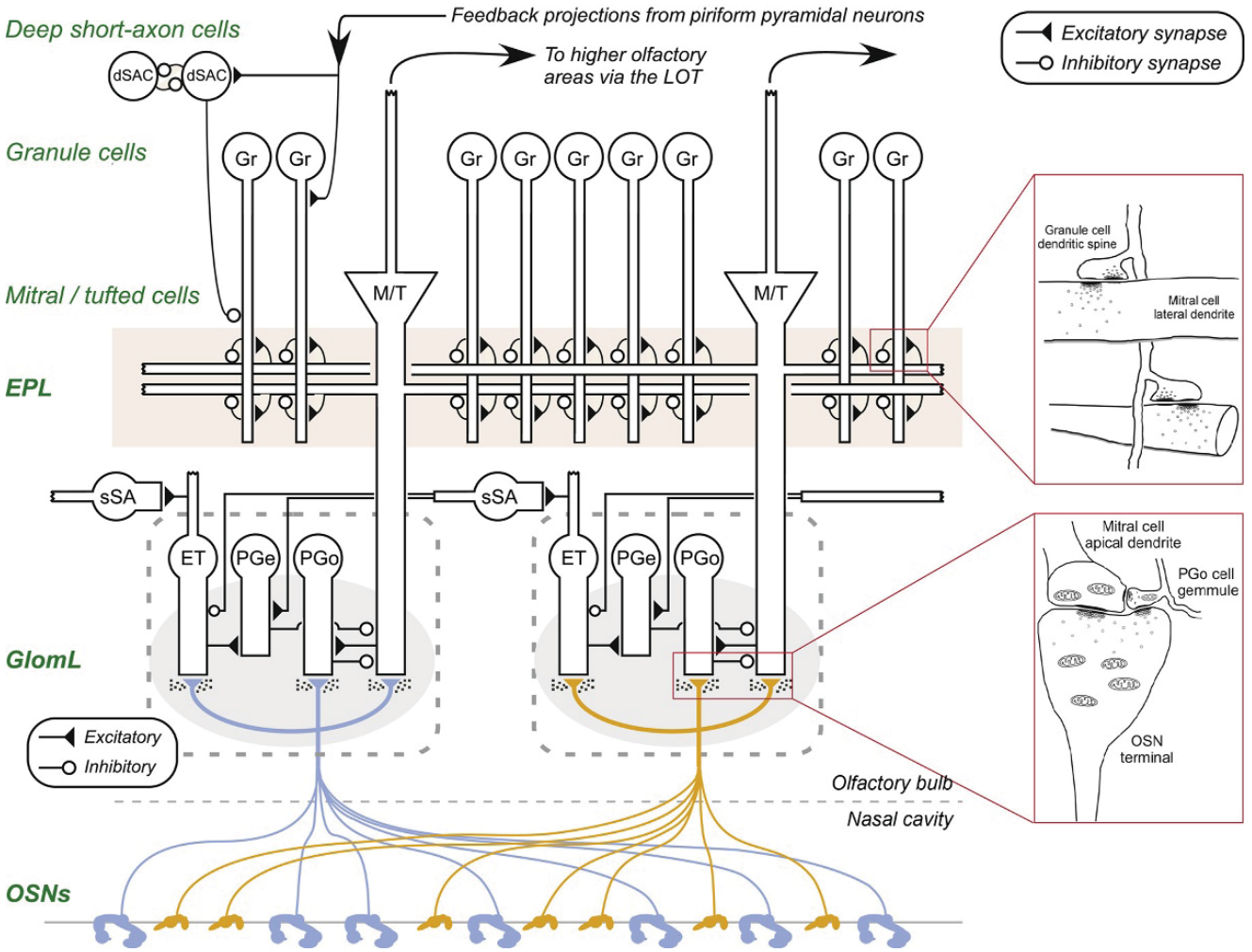


**FIGURE 1**

Connections of the olfactory bulb neuronal network. Circuit diagram of the mammalian olfactory bulb. The axons of olfactory sensory neurons expressing the same odorant receptor type converge together as they cross into the brain and arborize together to form glomeruli (shaded ovals) across the surface of the olfactory bulb. Several classes of olfactory bulb neuron innervate each glomerulus. Interneurons include olfactory nerve-driven periglomerular cells (PGo), external tufted cell-driven periglomerular cells (PGe), and multiple subtypes of external tufted cells (ET). Superficial short-axon cells (sSA) are not associated with specific glomeruli but project broadly and laterally within the deep glomerular layer, interacting with glomerular interneurons. Principal neurons include mitral cells and tufted cells (collectively depicted as M/T), which interact via reciprocal connections in the external plexiform layer (EPL) with the dendrites of inhibitory granule cells (Gr), thereby receiving recurrent and lateral inhibition. Both of these principal neuron types project divergently to several regions of the brain. The heterogeneous deep short-axon

*(continued)*

tuning ranges of one to two orders of magnitude have been directly measured in dissociated OSNs (Duchamp-Viret et al., 1990a,b; Firestein and Shepherd, 1991; Firestein et al., 1993; Trotier, 1994). The concentrations of naturally encountered odorants, of course, vary much more widely than this. Consequently, odor quality information contained in the relative activation levels among OSN classes would be inconsistent across concentrations, as various ORs in the activated ensemble approach their activation ceilings or floors and disrupt the ratiometric, and ultimately even the ordinal, profile of OSN activation levels (Cleland et al., 2011). The absence of reliable diagnostic features of odor quality within OSN activity profiles would, of course, render the olfactory system unable to distinguish odors effectively, at least outside of narrow concentration windows. Yet, it is clear that olfactory systems are able to resolve this conundrum.

This problem is surprisingly difficult to solve owing to the many unavoidable nonlinearities inherent to the transduction process. Indeed, it is likely that no one solution could do so reliably. Instead, it has been proposed that the mammalian olfactory system uses several (at least six) computational mechanisms in series to progressively reduce the concentration-dependent variance in odor representations such that different concentrations of odors evoke reasonably similar representations, while preserving the variance arising from differences in odor quality (Cleland et al., 2011). Briefly, these include adaptive sampling behaviors (e.g., regulating odor concentration in the nose by adjusting the strength of sniffing), the diversification of concentration tuning among sister OSNs via receptor reserve so as to generate broader aggregate dose–response curves in glomeruli, intensity compression at the output synapses of OSNs, adaptation to background at this same synapse, and at least two computations in postglomerular olfactory bulb circuitry including feedback-dependent normalization of activity and, finally, learning-dependent categorical

**FIGURE 1—Cont'd** cell population (dSAC) includes cells that deliver GABAergic inhibition onto granule cells and one another, and, along with granule cells, receive centrifugal cortical input from piriform pyramidal cells. OE, olfactory epithelium (in the nasal cavity); GL, glomerular layer; EPL, external plexiform layer; MCL, mitral cell layer; IPL, internal plexiform layer; GCL, granule cell layer. Filled triangles denote excitatory synapses; open circles denote inhibitory synapses. Note that sSA to PG synapses are depicted as excitatory despite being GABAergic (see text), and sSA to sSA synapses exist but are not depicted. *Upper right inset.* Illustration of the mitral–granule synapses in the external plexiform layer (EPL) that mediate recurrent and lateral inhibition. Mitral cell lateral dendrites excite granule cell spines, and granule cells inhibit mitral cell lateral dendrites. This synaptic circuit is the basis for recurrent and lateral inhibition across the olfactory bulb and mediates the generation and coordination of gamma oscillations. *Lower right inset.* Illustration of the triune synapse at which an OSN excites a mitral cell and PGo cell gemmule (spine) in parallel, and the PGo cell immediately inhibits the mitral cell. This synaptic triad is the basis for nontopographical intraglomerular inhibition proposed to mediate contrast enhancement in the olfactory system (see text).

*Figure adapted from Cleland (2010).*

binding across remaining differences in the representations of the same odorant at different concentrations. Among the preglomerular mechanisms, the most computationally interesting is the putative use of receptor reserve to diversify the concentration tuning of sister OSNs. Receptor reserve, or spare receptor capacity, is a phenomenon that arises in metabotropic receptor systems when the capacity of the receptors to generate second messenger substantially exceeds the capacity of the coupled effector systems to respond to these high levels of second messenger. In such a system, near-maximal effector activation can be achieved with an arbitrarily small proportion of ligand–receptor binding. That is, the concentration of odor ligand evoking half-activation of the OSN (i.e., its $EC_{50}$) can be arbitrarily lower than the dissociation constant ($K_d$) of the ligand–receptor interaction. If utilized in OSNs, receptor reserve can explain how the olfactory system—in some species more than others—is able to detect extremely low concentrations of odorants despite utilizing ORs that exhibit modest dissociation constants for most ligands. Second, if the sister OSNs of a convergent population express a distribution of different degrees of receptor reserve, and hence exhibit different concentration tuning curves (for the same odor ligands), then the convergent population as a whole will exhibit an arbitrarily broadened aggregate dose–response curve (Cleland and Linster, 1999). Because all sister OSNs converge onto one or two glomeruli on the surface of the olfactory bulb, the collective presynaptic activity within each glomerulus could express these broad dose–response curves. Indeed, imaging studies of glomerular activation profiles show that they do exhibit dose–response curves that are much broader than those of individual OSNs, responding to ligand concentrations across several orders of magnitude (Friedrich and Korsching, 1997; Wachowiak et al., 2002). Such broad dose–response curves produce wide quasilinear ranges in which the pattern of relative levels of activation across many activated glomeruli, nominally diagnostic for a given odorant, can be roughly maintained. These principles illustrate the sophistication of odor sampling mechanisms at even the most peripheral stage, indicating how OSN properties can take advantage of physical laws to increase their collective coding capacity and reduce the computational burden on subsequent processing stages.

## 3 ODOR REPRESENTATIONS

The presynaptic pattern of activation of OSNs generated by a given stimulus—essentially equivalent to the pattern of activation of glomeruli on the surface of the olfactory bulb—is referred to herein as the *primary olfactory representation*. Briefly, it contains all of the information that the OSN population has transduced from the environment, while also incorporating the nonlinearities and computations of the OSN layer as they are presented—in the form of spike trains from millions of OSNs converging onto hundreds of glomeruli—to the input circuitry of the olfactory bulb. (As the imaging of activity in the glomerular layer predominantly measures activity within OSN arbors, the primary olfactory representation also is relatively straightforward to visualize experimentally). While this representation certainly

reflects the quality of environmental odors, it is important to realize that the two are not the same. Even at this early stage, the neural representation has emphasized some environmental features at the cost of others and has discarded certain forms of stimulus variation because it does not have the physical capacity to record them accurately. This fundamental process is repeated again and again in the sensory cascade, as every level of processing transforms the information in a way that is not specifically *accurate* so much as it is *useful*—at each stage discarding or deemphasizing some sensory information in favor of information that is more likely to be of interest.

For clarity, this sensory cascade can be conceived of as a *succession of representations*, each of which samples from the previous representation as its input. For example, if the OSN arbors constitute the primary representation, then the pattern of activity across the second-order principal neurons of the olfactory bulb (mitral and tufted cells) can be thought of as the secondary representation. Importantly, in the present context, the word "representation" is used concretely to refer to the sensory information embedded in neural activity patterns along with the metrics used by those neurons to embed this information. If we describe the activation level of each glomerulus with a value from 0 (inactive) to 1 (maximally active), then any odor representation—any possible pattern of OSN activation—can be mapped as a single high-dimensional unit vector. That is, with each OR-specific glomerulus constituting an independent dimension (counting sister glomeruli as one), a mouse olfactory bulb maps out a roughly 1000-dimensional space (~350-dimensional for humans), into which—under idealized circumstances—any odor representation can be unambiguously mapped as a single point.

## 4 SIMILARITY SPACES

In the real world, of course, it is not quite so simple. No two stimuli are ever identical—even a second sniff of the same odor in the same environment will yield small differences in the patterns of odorous molecules binding to ORs. More interestingly, different instantiations of "the same" odor—such as two different oranges, perhaps from different trees, or with one more ripe than the other—produce similar but not identical odors. Mapping each of these "orange" odors into our 1000-dimensional space would produce a different point for each one, clustered together in a high-dimensional cloud of neighboring points. There likely would be more variability in some dimensions of this cloud than in others (corresponding to those ORs/glomeruli that are more sensitive to the small differences among these different orange odors), thereby producing a cloud with an irregular shape. This cloud defines a region within this 1000-dimensional space delimiting the odor qualities that are recognized as "orange"—that is, a range of variability in odor quality that all is categorized and recognized as the odor of orange. These clouds define a nonuniform distribution of odors within olfactory similarity space (Castro et al., 2013), and each can be referred to as describing the size and shape of an odor representation.

An important property of this high-dimensional space is that it is a *similarity space*, in which proximity in the space is related to odor similarity. Similarity spaces are a staple of sensory systems and often are clearly and directly reflected in the brain. For example, the one-dimensional similarity space of auditory spectral frequency is reflected in the tonotopic organization of the cochlear nucleus—that is, neighboring tone frequencies are perceptually similar and activate correspondingly neighboring populations of neurons within the nucleus. Similarly, the retinotopic localization of visual stimuli can be mapped two-dimensionally; photoreceptors and retinal ganglion cells that are physical neighbors also have correspondingly similar or overlapping spatial receptive fields. What is the olfactory analogue of these similarity relationships among elemental stimulus properties, and how might they be mapped within the olfactory bulb?

ORs respond strongly not only to preferred odorants but also to structurally similar odorants, including similar aliphatic molecules with slightly different carbon chain lengths (neighbors in *homologous series* of odorants) as well as several side-chain and multiple-bond variants (Araneda et al., 2000). These arbitrary but consistent receptive fields of ORs form the physical foundation of olfactory perceptual space (Zaidi et al., 2013), in that two odors that activate largely overlapping sets of ORs tend to smell correspondingly similar (Cleland et al., 2002). Unlike retinal cones or auditory hair cells, however, these receptive fields lack any external basis for quantitative similarity other than the probability of coactivation. The most important consequence of this fact is that the quantitative similarity between the receptive fields of two different ORs is not fixed but depends upon the statistical structure of the odor environment. (For example, two ORs may have essentially identical receptive fields, and hence be functionally 100% redundant, until the day comes when a new odor is encountered that activates one OR and not the other). For this reason, the receptive fields of different ORs must be considered independent in this context, such that the full dimensionality of odor space equals at least the number of different OR types. Note that in any given finite universe of odorants, the dimensionality of odor space can be reduced, often substantially (Haddad et al., 2010; Koulakov et al., 2011). However, this lowered dimensionality reflects the relative poverty of the input space used in the study rather than any property of the system *per se*. If the olfactory system is to be able to interpret any possible combination of receptor inputs received, then a high-dimensional input space is unavoidable, and the neural circuitry of the system must accommodate this fact.

# 5 GLOMERULAR LAYER COMPUTATIONS

## 5.1 Sideband Suppression: A Problem of Dimensionality

One of the early transformations of sensory representations in many modalities is sideband suppression, otherwise known as contrast enhancement or edge enhancement. This on-center/inhibitory surround, or Mexican-hat, transformation sharpens

sensory representations by selectively inhibiting neurons on the periphery of the representation—for example, the edges of a retinal image—in order to enhance the figure-background contrast of the representation. In most sensory systems studied to date, this transformation is mediated by lateral inhibitory projections. Crucially, however, the effectiveness of lateral inhibition in this context depends upon the topographical mapping of stimulus similarity, such that neurons with similar receptive fields are located correspondingly physically closely to one another within the relevant brain region. In the retina, for example, physically neighboring neurons mediate similar sensory information because overlapping regions of the visual field are sampled by adjacent photoreceptors. In the cochlear nucleus and other auditory regions, one-dimensional tonotopic maps ensure that physically neighboring neurons will encode similar sound frequencies. Both systems follow the same organizational principle: the physical proximity of neurons reflects the similarity of their receptive fields. Consequently, the projection of inhibition by neurons onto their physical neighbors is an effective means of projecting inhibition onto those neurons that mediate similar sensory information. The spatial contrast of visual images therefore can be enhanced by lateral inhibitory projections within the two dimensions of the retina (Cook and McReynolds, 1998) and tuning in the auditory system can be similarly sharpened along the single dimension of frequency (Suga et al., 1997; Yang et al., 1992).

Nearest-neighbor lateral inhibition is effective as a mechanism of contrast enhancement in these two modalities only because they are both low-dimensional. Specifically, as neural cortices are layered structures, and thus functionally two-dimensional, nearest-neighbor lateral inhibition is effective only for modalities in which the similarity space can be mapped continuously onto two or fewer dimensions. Attempts to map additional dimensions of similarity onto lower dimensional surfaces necessarily result in discontinuities (Kohonen and Hari, 1999), as can be seen, for example, in primary visual cortex, where the mapping of both retinotopy and orientation onto the same surface produces the discontinuous map elements known as pinwheels embedded within a broad, inherited retinotopy (Bressloff and Cowan, 2003). In the case of olfaction, projecting a similarity space with hundreds of dimensions onto the two-dimensional surface of the olfactory bulb has a more extreme fragmenting effect—effectively producing a complete discretization of input qualities (receptive fields) that manifests physically as glomeruli. This extreme discretization is qualitatively different from the continuous layers observed in other sensory cortices, even when those cortices exhibit prominent receptive field discontinuities; for example, primary visual cortex, and also primary somatosensory cortex, in which the discontinuities in body surface representation illustrated by the somatosensory homunculus reflect the projection of the two dimensions of the body surface onto a single dimension mapped coronally along the cortical surface (Penfield and Rasmussen, 1950). This corroborates the theoretical finding that olfactory similarity space is far too high-dimensional to be mapped continuously onto the olfactory bulb surface.

Graded similarity in perception exists in olfaction, of course. Odors can be perceived as more or less similar to one another, and this perceptual similarity can be

measured behaviorally (Cleland et al., 2002). This similarity is related to the chemical structures of odorants and corresponds to the relative similarity of the patterns of activation levels across the population of ORs/glomeruli, as discussed above. Are there other principles of organization evident at this stage? Despite being theoretically ruled out by the high dimensionality of the input space, many efforts have been made to show that the position of discrete glomeruli onto the olfactory bulb surface reflects OR-receptive field similarity in some way (Johnson and Leon, 2007; Mori et al., 2006). For the purposes of similarity-dependent computations, it is clear that they do not; the physical locations of glomeruli are not predictive of their receptive fields (Soucy et al., 2009). That said, some deviations from uniformity have been observed in these patterns, notably a tendency for larger molecules to activate slightly more ventral populations of glomeruli in rodents (Fletcher et al., 2009; Johnson et al., 2009), probably because of the segregated mapping in the bulb of axonal arbors arising from central canal OSNs and those arising from OSNs located in the medial and lateral recesses of the olfactory turbinates (Schoenfeld and Cleland, 2005), and a small preference for glomeruli with very similar receptive fields to be immediately adjacent (Soucy et al., 2009), which may reflect recent gene duplication and divergence or other small differences that induce activity-dependent segregation during development (Strotmann and Breer, 2006). However, these interesting relationships do not affect the governing principle that glomerular proximity cannot reliably provide information on receptive field similarity. Finally, studies using lower resolution (spatially averaged) maps of glomerular activation patterns have tended to show broad differences in activation patterns that correlate with major chemical groups (albeit not always consistently among different laboratories). *A priori*, these results could reflect real differences and/or artifacts arising from low spatial resolution; for example, inactive glomeruli embedded within a region of active glomeruli are not recorded, which results in overestimation of the breadth and clustering of odor-evoked activity. Given that higher resolution maps of glomerular activation do not show these region-specific activation profiles, such resolution artifacts are likely to contribute to these findings. For the purposes of elucidating the cellular and network mechanisms underlying similarity-dependent computations, however, the critical point is that the proximity of glomeruli does not reliably predict the similarity or overlap of their receptive fields. This consequence of high dimensionality renders ineffective any computational mechanisms, such as nearest-neighbor lateral inhibition, that rely on physical proximity as a proxy for receptive field similarity. Alternative solutions are required.

## 5.2 Nontopographical Contrast Enhancement

The transformation between the primary odor representation and the secondary odor representation clearly effects contrast enhancement (Yokoi et al., 1995). Unlike the chemoreceptive fields of OSNs, or their aggregates within glomeruli, the chemoreceptive fields of mitral cells (second-order principal neurons; Fig. 1) exhibit clear surround inhibition, in which the surround is defined in terms of chemical and

perceptual similarity (Fig. 2). However, because of the discretized and nontopographically organized representation of olfactory stimulus similarity across the olfactory bulb, contrast enhancement transformations in this system cannot rely on physical proximity-based mechanisms such as center-surround lateral inhibition. Moreover, because olfactory similarity lacks a simple, externally defined basis comparable to wavelength or pitch, any algorithms that depend on durable interglomerular inhibitory projections will lose effectiveness whenever the odor environment changes. These limitations can be resolved by a mechanism, *nontopographical*

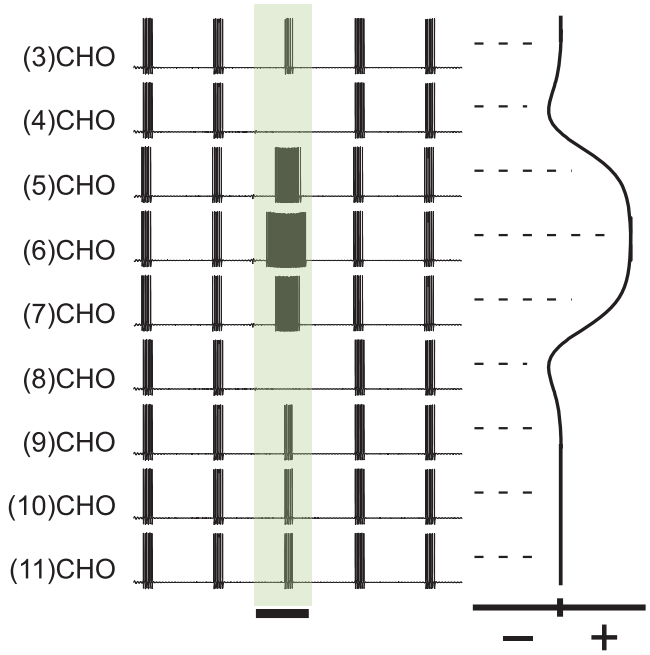


**FIGURE 2**

Nontopographical contrast enhancement. Replication of experimental data from Yokoi et al. (1995) by the NTCE computational model (Cleland and Sethupathy, 2006) demonstrating on-center/inhibitory-surround decorrelation in mitral cells by recording from a single rabbit mitral cell *in vivo* during the presentations of nine sequentially similar odorants (3-carbon through 11-carbon aliphatic aldehydes). Periodic bursts of spikes reflect background mitral cell activity evoked by the respiration cycle. A 2-s odorant stimulus was presented during the third inhalation (black bar; shading). The odorant hexanal [(6)CHO] is near the center of this mitral cell's receptive field and evokes the strongest activation; pentanal [(5)CHO] and heptanal [(7)CHO] also excite the cell, whereas butanal [(4)CHO] and octanal [(8)CHO] are within its inhibitory surround, and hence evoke a net inhibition. The mitral cell is unresponsive to the other four odorants. The curve to the right illustrates how the "Mexican-hat" function maps onto the trajectory through odor similarity space defined by the homologous odor series. The plus sign denotes excitation; the minus sign denotes inhibition.

*Figure adapted from Cleland (2010).*

*contrast enhancement* (NTCE), that is based upon intraglomerular feed-forward inhibition and nonspecific feedback normalization within the glomerular layer (Cleland, 2010; Cleland and Sethupathy, 2006; Cleland et al., 2007). In addition to enabling contrast enhancement in a high-dimensional modality such as olfaction, this nontopographical mechanism does not require a built-in foreknowledge of the similarities in receptive fields exhibited by different ORs/glomeruli in order to distribute inhibition correctly and is entirely independent of the physical location of glomeruli within the olfactory bulb. Briefly, OSN axonal arbors in each glomerulus deliver glutamatergic excitation onto mitral cell dendrites as well as the dendritic spines of local inhibitory neurons known as periglomerular cells (specifically, the PGo subtype; Shao et al., 2009; Fig. 1, *lower inset*). These periglomerular cell spines directly deliver $GABA_A$-ergic shunt inhibition onto mitral cell dendrites in parallel to the excitatory inputs that the latter receive from OSNs (Shao et al., 2013). Theoretical models indicate that this configuration effects contrast enhancement with respect to a similarity space that is naturally inherited from the current chemosensory environment. Specifically, mitral cells associated with a given odorant receptor are excited only by the odor ligands with the highest affinity (relative to the activated population), which activate the mitral cell strongly enough to overcome this parallel feed-forward inhibition. In response to lesser degrees of OSN activation—that is, the *surround* with respect to odorant receptor binding potency (Fig. 3)—PGo-mediated feed-forward inhibition dominates direct excitation, such that mitral cells exhibit a subbaseline inhibitory response (Fig. 2). Recordings from olfactory bulb slices have since demonstrated that feed-forward shunt inhibition by periglomerular cells is able to prevent spiking in mitral cells given moderate levels of afferent input (Gire and Schoppa, 2009). Finally, minimal levels of afferent activation activate neither mitral cells nor feed-forward inhibition appreciably. As a result of this transformation, odor-evoked activity patterns across mitral cell ensembles (secondary representations) are sparser and less overlapping than are the corresponding primary representations observed among OSNs and glomeruli. Furthermore, the stringency of this contrast-enhancing transformation can be regulated by centrifugal neuromodulatory inputs, specifically including inputs mediated by nicotinic cholinergic receptors in the glomerular layer (Castillo et al., 1999; D'Souza and Vijayaraghavan, 2012; Li and Cleland, 2013; Mandairon et al., 2006). Critically, contrast enhancement by this mechanism does not require any specific lateral inhibitory projections within the olfactory bulb or any particular proximity relationships among glomeruli. The physicochemical properties of odorants can be represented in olfactory bulb circuitry without the need for any higher level of organization among glomeruli.

## 5.3 Feedback Normalization

The NTCE algorithm as presented above has one major limitation: concentration. In general, higher stimulus intensities both increase the activity of activated primary sensory neurons and broaden the neural response by recruiting additional, more

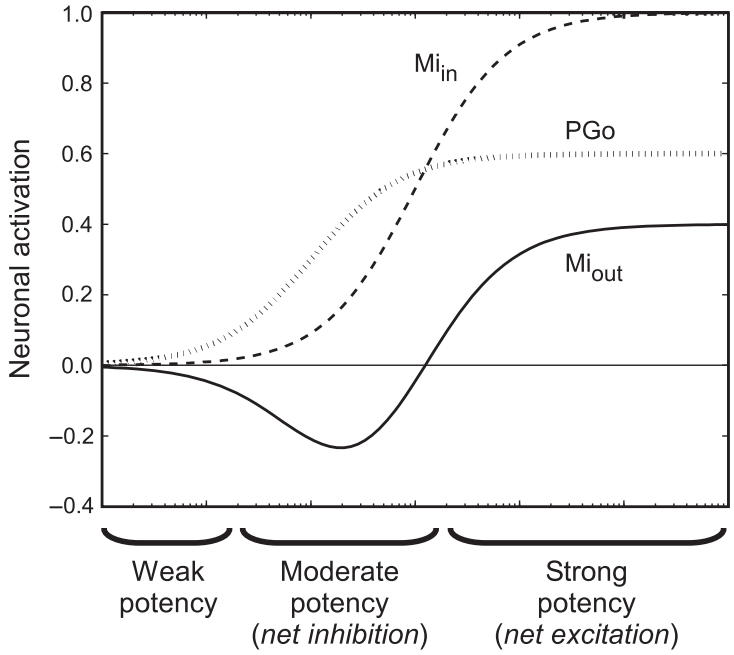


**FIGURE 3**

Nontopographical contrast enhancement. Illustration of the nontopographical contrast enhancement model. The levels of activation of selected MOB neurons from a single glomerulus are depicted as a function of the activation of its corresponding OSN population (ligand–receptor potency). Negative values of neuronal activation denote inhibition. Odors with very weak potencies for the OR in question evoke no OSN activity and hence no mitral cell activity. Increasing the ligand–receptor potency to the point where it evokes OSN activity begins to excite PGo neurons, which, owing to their high input resistance and small spine volume, respond strongly even to weak inputs and deliver local intraglomerular inhibition onto mitral cells. Moderate ligand–receptor potencies begin to also directly activate mitral cells ($Mi_{in}$), but this excitation is overpowered by the inhibition received from the more strongly activated PGo neurons, which shunts away depolarizing current such that the overall net response of mitral cells ($Mi_{out}$) is inhibitory. Strong ligand–receptor potencies excite mitral cells more strongly, overwhelming the capacity of PGo inhibition to impair spike generation and hence evoking action potentials in mitral cells. The result is that mitral cells exhibit an excitatory response to high-potency odorant ligands and an inhibitory response to odorant ligands of moderate potency—that is, to the "surrounding" region in a space defined by odor quality.

*Figure adapted from Cleland and Sethupathy (2006).*

weakly tuned primary sensory neurons into the activated ensemble. In the olfactory system, this corresponds to increased probabilities of ligand–receptor binding as ligand concentration rises, eventually binding significantly even to receptors for which the ligand in question has very low affinities. Hence, as odor concentrations rise, an increasingly broad range of OSNs become activated, substantially broadening the primary representation. Moreover, as illustrated in Fig. 3, this increased

binding of each OR type would mimic higher ligand–receptor affinities, ultimately bypassing the net inhibitory region of that relationship as the cellular input activation levels depicted on the abscissa are increased simultaneously in all glomeruli. Accordingly, some form of feedback normalization is necessary in order to rescue the effectiveness of the NTCE algorithm across odor concentrations.

Normalization processes in sensory systems are widespread across sensory modalities and are essential for segregating quality from concentration effects and for constructing intensity-independent representations of stimulus quality (Cleland et al., 2011). In principle, robust intensity normalization processes require global feedback inhibition, in which uniform inhibition is delivered to all units in proportion to the mean activity level of all sensory inputs. In the olfactory system, this normalization has been proposed to rely upon a broad lateral network formed by external tufted and superficial short-axon (sSA) cells in the glomerular layer of the olfactory bulb (the ET/sSA network; Fig. 4). Briefly, this widespread, highly interconnected lateral network (Fig. 4) is activated by direct OSN excitation of external tufted cells within glomeruli (Fig. 1). The lateral network integrates these heterogeneous activation levels across the bulbar input layer and delivers a uniform, "averaged" level of excitation onto PGe-type periglomerular cells in all glomeruli, which in turn inhibit their local mitral cells (Fig. 1). Owing to small-world network effects, the feedback inhibition delivered by models of this network is approximately uniform across the olfactory bulb (Fig. 5), despite the fact that the ET/sSA network predominantly exhibits a localized, center-surround morphological profile (Fig. 4). This small-world effect conserves substantial volume and metabolic resources compared with a truly all-to-all feedback inhibitory network; when implemented in neuromorphic hardware, this circuit saved over 90% of the energy costs of a fully connected feedback network (Imam et al., 2012). The result of this computation, manifested in the pattern of afferent input to mitral cells, is a preservation of relative activity levels among glomeruli across a broad range of absolute stimulus intensities (Cleland, 2010; Cleland et al., 2007).

Interestingly, this normalization model originally was built on the premise that sSA cells, which are responsible for the long-distance lateral projections, are excitatory (Cleland et al., 2007). Initial physiological studies of these neurons had indicated that they were glutamatergic and excitatory (Aungst et al., 2003); however, subsequent studies demonstrated that they are GABAergic and dopaminergic (Liu et al., 2013), and indeed probably constitute one extreme of a single morphologically heterogeneous class of interneurons that includes periglomerular cells (Kiyokage et al., 2010; McGann, 2013; Sethupathy et al., 2013). This is interesting because recent work has shown that, despite their GABAergic phenotype, sSA cells are clearly the effectors of a functionally excitatory lateral network that results in the broad and graded inhibition of mitral cells (Marbach and Albeanu, 2011). This lateral excitatory effect across the sSA network potentially could arise via gap-junction coupling among sSA and periglomerular cells, or by rendering GABAergic synapses onto periglomerular and sSA cells excitatory owing to a reversed chloride gradient in these neurons. Indeed, a reversed chloride gradient resulting in GABA-mediated

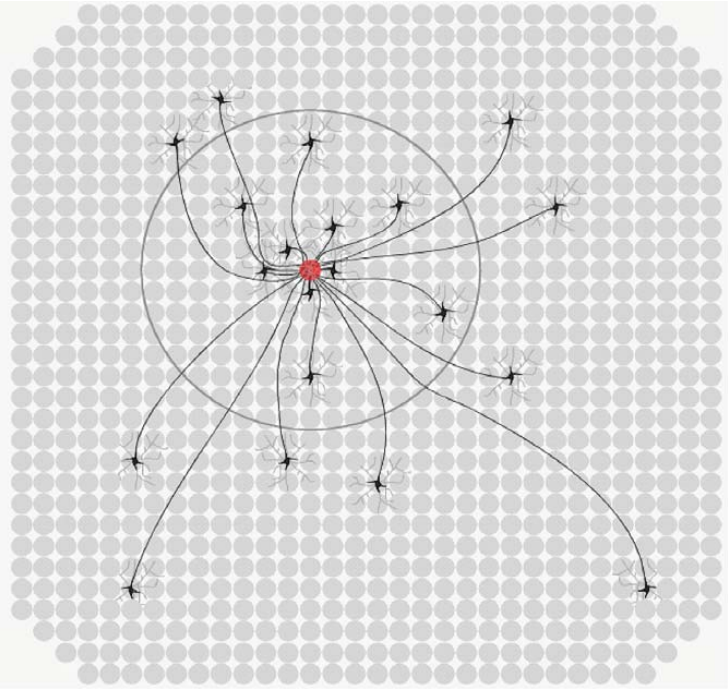

**FIGURE 4**

Global feedback normalization in the olfactory bulb glomerular layer. Statistically realistic schematic depiction of lateral connectivity in the deep glomerular layer via superficial short-axon (sSA) cells. One thousand glomeruli (gray circles) are depicted, illustrating the full glomerular diversity of a mouse olfactory bulb. Dye injections into single glomeruli (red glomerulus near center) indicate that approximately 50 sSA neurons project axons to a given glomerulus. (Twenty sSA neurons are depicted here, and whereas sSA cell axons branch extensively, for clarity only one axonal branch per sSA neuron is depicted here.) The dendritic arbors of sSA neurons extend across a small number of glomeruli (depicted as light gray arbors around each sSA soma). Of the sSA neurons projecting axons to a given glomerulus, 50% are located over 5–7 glomerular diameters away from the injected glomerulus (region denoted by a large circle), whereas 10% are located over 15–18 glomerular diameters distant. The longest sSA axons (not shown) extend 20–30 glomerular diameters, an appreciable fraction of the circumference of the MOB. Despite this apparent center-surround topology, simulations of this network exhibit small-world effects and deliver uniform feedback inhibition to all glomeruli; recent experimental data support this model (see text).

*Data from Aungst et al. (2003). Figure adapted from Cleland (2010).*

excitation has been reported in adult mouse periglomerular cells in another context (Parsa et al., 2011), though its potential effect on global feedback normalization has not yet been studied.

The functional normalization of mitral cell activity levels also is observable *in vivo*. Mitral cell responses to increasing odorant concentrations differ; that is,

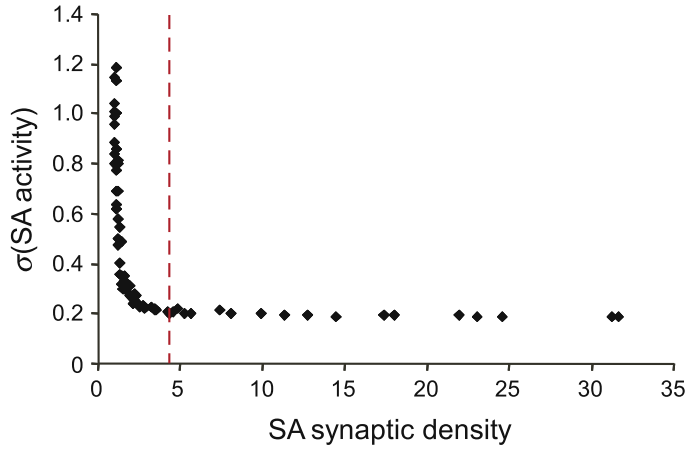


**FIGURE 5**

Global feedback normalization in the olfactory bulb glomerular layer. The morphologically center-surround interglomerular connectivity of the ET/sSA network is functionally equivalent to a fully connected all-to-all network. The abscissa denotes an overall measure of sSA network connectivity between the hypothetical extremes of no ET/sSA connectivity at all (fully isolated glomeruli) and full connectivity in which every glomerulus is directly linked to every other glomerulus (all-to-all connections; see Cleland et al. (2007) for details). The greater the connectivity, the lower the variance in the activation levels among sSA neurons. Zero connectivity means that sSA neurons directly inherit (via ET cells) the heterogeneous odor-evoked activation levels of the OSNs associated with the nearest glomerulus, causing different sSA neurons to differ widely in their activation levels across the MOB. By contrast, full connectivity implies that every sSA neuron receives essentially the same amount of afferent input (by receiving excitation drawn from every glomerulus in the MOB), yielding minimal variance in activity levels among different sSA neurons. An estimate of actual ET/sSA connectivity in the mouse MOB by Aungst et al. (2003) (dashed vertical line; see Fig. 4) suggests that this center–surround connectivity pattern exerts the same quantitative, globally uniform normalizing effect as would a fully connected all-to-all network, but at a fraction of the metabolic cost, owing to small-world network effects.

*Figure adapted from Cleland et al. (2007).*

individual mitral cells might either increase or reduce their response levels, or may transition from net excitation to inhibition, or vice versa (Harrison and Scott, 1986; Meredith, 1986; Wellis et al., 1989). They do tend to exhibit shorter response latencies in response to higher odorant concentrations, but do not exhibit reliably monotonic increases in activation levels comparable to those observed in individual OSNs or populations of convergent OSNs. That is, some form of normalization process is clearly active between the primary representation across the OSN population and the secondary representation composed of mitral cell spiking activity patterns. As a result, mitral cell responses are maintained within a relatively narrow band of absolute activation levels. Such tight control over absolute activation levels is convenient for

downstream neuronal processing, as the dynamic range of synaptic responses in follower cells is fundamentally limited. However, this does suggest that the main metric of information content in mitral cell response patterns may no longer be based on absolute activation levels *per se*.

# 6 DEEP-LAYER COMPUTATIONS

## 6.1 The External Plexiform Layer

Insofar as it has been described above, the secondary odor representation of mitral cells is essentially a contrast-enhanced and normalized version of the primary representation that has taken advantage of the early computations enabling some preservation of activity ratios among glomeruli across concentrations in that representation. Subsequent glomerular layer feedback normalization has substantially reduced the differences in raw activation levels among mitral cells compared to the wide range exhibited by the primary representation. What now are the effects of the prominent lateral network embedded within the external plexiform layer (EPL; Fig. 1), in which the lateral (secondary) dendrites of mitral cells excite the dendritic spines of GABAergic granule cells and are in turn inhibited by those granule cell spines (Fig. 1, *upper inset*)? Along with the recurrent self-inhibition of mitral cells, the distribution of mitral–granule interactions effects a broad lateral inhibitory network extending across the entire OB, by which activity in some mitral cells can inhibit activity in other mitral cells. While this EPL lateral inhibitory circuit has received substantial attention in the literature, its effects on mitral cell activity and its overall role in odor processing remain relatively unclear.

The classical interpretation suggested that olfactory contrast enhancement was mediated in the EPL via nearest-neighbor lateral inhibition, as occurs in lateral inhibitory networks in other, lower dimensional modalities (Rall and Shepherd, 1968; Yokoi et al., 1995). This hypothesis is now clearly ruled out. Not only do mitral cells exhibit receptive fields that do not correspond to their relative locations (Soucy et al., 2009), but the distribution of lateral inhibitory weights measured between mitral cells is spatially dispersed and does not respect neighborhood relationships (Fantana et al., 2008). These physiological results corroborate data using transsynaptic tracers believed to reflect synaptic weights, which also indicate a sparse matrix of EPL connections among widely distributed glomerular columns (Kim et al., 2011; Willhite et al., 2006); *column* here refers to the bulbar circuitry descending directly from a given glomerulus. The EPL certainly is a lateral inhibitory network; however, unlike nearest-neighbor lateral inhibitory systems in other modalities, it does not respect physical proximity in its distribution of synaptic efficacies. Instead, it appears to map a virtual neighborhood of arbitrary dimensionality, suggesting that it can perform meaningful transformations upon high-dimensional odor representations.

Despite this potential, it is unlikely that EPL interactions can decorrelate OSN receptive fields as do glomerular networks because the necessary information

regarding receptive field similarity is unavailable to the EPL network. Specifically, the periglomerular cell-mediated feed-forward inhibition that effects the inhibitory surround in glomerular layer circuitry does not extend to the EPL (Fig. 1). It is tempting to hypothesize instead that different glomerular columns exhibiting similar receptive fields, irrespective of location, selectively inhibit one another in a high-dimensional variant of traditional lateral inhibitory networks (as has been modeled in honeybees by Linster et al., 2005), but in fact the receptive fields of the sparsely distributed glomerular columns that contribute to the response of a given mitral cell are not related (Fantana et al., 2008). Moreover, such a hypothesis suffers from two crippling theoretical contraindications. First of these is the problem of how such a selective, point-to-point map of synaptic weights appropriate to the task could be constructed. Ruling out the idea that quantitative measures of overlap among each of the receptive fields of ORs expressed in OSNs could somehow be genetically encoded within mitral cells, activity-dependence is the only remaining solution, and this is impaired by the absence of an adequate training set. Genuinely elemental odorant stimuli do not exist. Any odorant molecule will associate with and activate a number of different OR types (and hence glomerular columns), sometimes reflecting similarities in their receptive fields, but sometimes not, because multiple structurally unrelated epitopes on any given molecule are simultaneously available for binding whenever that odorant is presented. The consequence is that correlations in activity that in principle might serve to train EPL lateral inhibitory weights do not reliably reflect OR-receptive field similarities; consequently, the EPL cannot learn to perform similarity-dependent transformations of odor representations akin to those mediated in the glomerular layer. The second problem, as discussed above, is that the quantitative relationships among OR-receptive fields are not fixed, but depend upon the statistics of the odor environment. Specifically, the quantitative similarity between the receptive fields of any two ORs depends on the likelihood of their coactivation, which in turn depends on the unpredictable distribution of odorant epitopes in the immediate environment. These shifting natural scene statistics render EPL-based receptive field decorrelation unworkable, though they do not interfere with glomerular self-surround decorrelation, in which the inhibitory surround is derived directly from single OR-receptive fields rather than from the interrelationships among multiple such receptive fields.

## 6.2 Higher Order Organizational Principles

What, then, might be the role of a dense lateral inhibitory network such as the EPL that cannot be mapped onto the properties of primary receptive fields? The EPL is theoretically capable of an arbitrarily high-dimensional decorrelation of odor representations, but lacks a similarity space in which to base these computations. An exciting possibility is that there is no such fixed space at the EPL level. More precisely, if transformations based on elemental odor similarities are completed within the glomerular layer, then the EPL inherits those transformations (as primary visual cortex inherits retinotopy), but its own role instead is to retransform these odor

representations with respect to distinct, similarity-independent, higher-order bases derived from experience. Intrinsic learning mechanisms within olfactory bulb are well established; learning on longer timescales, in particular, depends on the odor-specific differentiation and incorporation of new granule cells into the EPL network (Lepousez et al., 2013; Chapter 6), and this adult neurogenesis in the OB is required for rats to learn to distinguish highly similar odorants that they do not spontaneously discriminate (Moreno et al., 2009). The implication is that EPL computations may underlie the remapping of odor space based on experience and learned utility, binding together sets of activated columns that together are diagnostic for a given odorant, and allocating resources to differentiate among similar odorants with different implications while grouping together ranges of related odors (i.e., regions of olfactory similarity space) associated with the same outcome or meaning. Indeed, learning is well known to progressively sharpen olfactory generalization gradients—the behavioral measurement of the size and shape of odor representations—and the breadth of such learned gradients also is sensitive to the real-world variance in quality exhibited by a learned odorant (Cleland et al., 2009, 2011). That is, through learning, the internal odor representation progressively adapts to reflect the real external quality variance of the learned odor. Such conditional remapping of selected regions of stimulus space is an emerging general property of sensory systems, reflecting the selective allocation of sensory/metabolic resources to different regions of peripherally defined similarity spaces, whether directly based on primary receptor distributions (as illustrated by the somatosensory homunculus) or on the higher order statistics of natural scenes (Olshausen and Field, 2004), though in olfaction this mapping may be particularly dependent on individual learning rather than species-specific priors. These hypotheses remain to be tested in olfaction, though pattern completion studies in piriform cortex (Wilson, 2009) suggest that a coordinated integration between the olfactory bulb as decorrelator and the piriform cortex as pattern integrator could serve this function, as also has been suggested by computational modeling studies (de Almeida et al., 2013; Hasselmo et al., 1992). Interestingly, these roles are similar to those proposed for the dentate gyrus and CA1 regions of the hippocampus (Sahay et al., 2011).

## 6.3 Transformation in Timescale

In addition to decorrelating and normalizing afferent representations, the OB appears to effect a transformation in timescale at the secondary representation; that is, to increase the degree of precision in spike timing that is relevant for information content. Absolute spike rates in mitral cells are not particularly diagnostic of columnar excitation levels, nor of odor quality information, whereas spike timing properties in this layer do carry this information (Lepousez and Lledo, 2013). The existence of spike timing regulatory mechanisms in olfactory bulb is clear. Whereas spike trains from hundreds of convergent OSNs are integrated over tens to hundreds of milliseconds in an actively sniffing animal, resulting in a time constant of mitral cell activation on the order of 50 ms in rats (Ennis et al., 1998), spike timing precision in mitral cells and

the cortical networks to which they project is on the order of milliseconds, coordinated by synchronized interactions in the beta (15–35 Hz) and gamma bands (40–100 Hz). Such coordinated spike timings underlie a new, faster-timescale metric for representing odor properties, presumably interpretable by follower cells possibly exhibiting some form of spike time-dependent plasticity (Linster and Cleland, 2010). Lower overall spike rates also render such metrics more metabolically efficient than are slower-timescale rate codes. This transformation in timescale relies upon several elements of the OB network that exhibit intrinsic temporal properties, including beta-band subthreshold oscillations in mitral cells (Desmaisons et al., 1999; Rubin and Cleland, 2006), intrinsic theta-band bursting in external tufted cells (Hayar et al., 2005; Liu and Shipley, 2008), and network-level oscillations both intrinsic to the olfactory bulb (gamma-band) and dependent on OB interactions with the piriform cortex (beta-band) (Kay et al., 2009). Modeling studies suggest that mitral cell subthreshold oscillations are reset in phase by inhibitory inputs, and that these inputs constrain the timing of spikes evoked by afferent excitatory input provided that this excitation is sufficiently slow in onset so as to not overpower the intrinsic dynamics of the mitral cell (Desmaisons et al., 1999; Li and Cleland, 2013; Rubin and Cleland, 2006). This inhibition-induced reset can be provided both by the same PGo cell inputs that effect self-surround decorrelation within glomeruli and by the granule cells that maintain EPL-based gamma oscillations in concert with mitral cells. The former input may serve to transiently synchronize activated mitral cells during sniffing, enabling a more rapid relaxation into EPL network synchrony than otherwise might be achieved (Timme et al., 2006), whereas the latter can maintain synchronous gamma oscillations across a population of differentially activated resonant mitral cells (Li and Cleland, 2013). The underlying mechanisms, interactions, and behavioral correlates of these diverse OB oscillators have been reviewed in detail elsewhere (Kay et al., 2009; Chapter 9).

## 6.4 Top-Down Regulation

Odor representations in the OB are not fixed. In addition to their probable transformation based on intrinsic learning mechanisms, they are regulated by ascending inputs from other brain regions, notably projections from the piriform cortex onto granule cells (which exhibit activity-dependent plasticity; Gao and Strowbridge, 2009) and multiple neuromodulatory centers including the horizontal limb of the diagonal band of Broca (HDB), the locus coeruleus, and the raphe nucleus. In particular, bulbar norepinephrine improves near-threshold olfactory sensitivity and signal-to-noise performance (Escanilla et al., 2010, 2012; Linster et al., 2011), mediates stress effects on odor memory (Manella et al., 2013), and may be necessary for intrinsic learning (Guerin et al., 2008; Moreno et al., 2012). Acetylcholine, normally released in the OB by fibers projecting from the HDB, has been shown to regulate the breadth of mitral cell receptive fields (Chaudhury et al., 2009; D'Souza and Vijayaraghavan, 2012) and to correspondingly sharpen perceptual generalization among similar odors in behavioral studies (Chaudhury et al., 2009;

Mandairon et al., 2006) via primarily nicotinic mechanisms, whereas bulbar muscarinic receptors affect inhibitory synaptic properties and the regulation of spike timing in the EPL (Li and Cleland, 2013; Pressler et al., 2007) and mediate key aspects of short-term odor memory (Devore et al., 2012; Ravel et al., 1994). The close apposition within second-order sensory neurons of the transduction of physical stimulus properties and the state-dependent neuromodulatory regulation of olfactory representations and odor learning is one of the great strengths of olfaction as a model system for representational learning and memory.

## 7 CONCLUSION

Olfactory sensory responses can be framed as a cascade of successive representations, each undergoing specific transformations that can be experimentally elucidated and theoretically modeled. The primary olfactory representation is mediated by OSNs and their convergent arbors in the olfactory bulb glomerular layer. This representation exhibits a strong sensitivity to odor concentration that can obscure the consistent representation of odor quality, a metabolically expensive rate-coding metric involving on the order of hundreds of thousands of densely spiking active neurons, and a direct dependence on the physical properties of odorant stimuli (moderated somewhat by the regulation of sniffing behavior). In contrast, the secondary olfactory representation, as mediated by mitral cells and propagated to several areas of the brain, is relatively weakly dependent on concentration, mediated by active ensembles comprising on the order of hundreds of relatively sparsely spiking neurons, and dependent on afferent OSN input, ascending corticobulbar projections, and extrinsic neuromodulation, as well as, most likely, intrinsic OB learning mechanisms. The transformations that construct the secondary olfactory representation from the primary are unusual among sensory systems both in their high dimensionality and the degree of their apparent plasticity. In sum, the OB implements a coordinated set of early sensory transformations directly analogous to those in other sensory systems, but accomplishes these with unique circuit architectures adapted to the properties of the olfactory modality.

## References

Araneda, R.C., Kini, A.D., Firestein, S., 2000. The molecular receptive range of an odorant receptor. Nat. Neurosci. 3, 1248–1255.

Aungst, J.L., Heyward, P.M., Puche, A.C., Karnup, S.V., Hayar, A., Szabo, G., Shipley, M.T., 2003. Centre-surround inhibition among olfactory bulb glomeruli. Nature 426, 623–629.

Bressloff, P.C., Cowan, J.D., 2003. A spherical model for orientation and spatial-frequency tuning in a cortical hypercolumn. Philos. Trans. R. Soc. Lond. B Biol. Sci. 358, 1643–1667.

Castillo, P.E., Carleton, A., Vincent, J.D., Lledo, P.M., 1999. Multiple and opposing roles of cholinergic transmission in the main olfactory bulb. J. Neurosci. 19, 9180–9191.

Castro, J.B., Ramanathan, A., Chennubhotla, C.S., 2013. Categorical dimensions of human odor descriptor space revealed by non-negative matrix factorization. PLoS One 8, e73289.
Chaudhury, D., Escanilla, O., Linster, C., 2009. Bulbar acetylcholine enhances neural and perceptual odor discrimination. J. Neurosci. 29, 52–60.
Chess, A., Simon, I., Cedar, H., Axel, R., 1994. Allelic inactivation regulates olfactory receptor gene expression. Cell 78, 823–834.
Cleland, T.A., 2010. Early transformations in odor representation. Trends Neurosci. 33, 130–139.
Cleland, T.A., Linster, C., 1999. Concentration tuning mediated by spare receptor capacity in olfactory sensory neurons: a theoretical study. Neural Comput. 11, 1673–1690.
Cleland, T.A., Sethupathy, P., 2006. Non-topographical contrast enhancement in the olfactory bulb. BMC Neurosci. 7, 7.
Cleland, T.A., Morse, A., Yue, E.L., Linster, C., 2002. Behavioral models of odor similarity. Behav. Neurosci. 116, 222–231.
Cleland, T.A., Johnson, B.A., Leon, M., Linster, C., 2007. Relational representation in the olfactory system. Proc. Natl. Acad. Sci. U. S. A. 104, 1953–1958.
Cleland, T.A., Narla, V.A., Boudadi, K., 2009. Multiple learning parameters differentially regulate olfactory generalization. Behav. Neurosci. 123, 26–35.
Cleland, T.A., Chen, S.Y., Hozer, K.W., Ukatu, H.N., Wong, K.J., Zheng, F., 2011. Sequential mechanisms underlying concentration invariance in biological olfaction. Front. Neuroeng. 4, 21.
Cook, P.B., McReynolds, J.S., 1998. Lateral inhibition in the inner retina is important for spatial tuning of ganglion cells. Nat. Neurosci. 1, 714–719.
de Almeida, L., Idiart, M., Linster, C., 2013. A model of cholinergic modulation in olfactory bulb and piriform cortex. J. Neurophysiol. 109, 1360–1377.
Desmaisons, D., Vincent, J.D., Lledo, P.M., 1999. Control of action potential timing by intrinsic subthreshold oscillations in olfactory bulb output neurons. J. Neurosci. 19, 10727–10737.
Devore, S., Manella, L.C., Linster, C., 2012. Blocking muscarinic receptors in the olfactory bulb impairs performance on an olfactory short-term memory task. Front. Behav. Neurosci. 6, 59.
D'Souza, R.D., Vijayaraghavan, S., 2012. Nicotinic receptor-mediated filtering of mitral cell responses to olfactory nerve inputs involves the alpha3beta4 subtype. J. Neurosci. 32, 3261–3266.
Duchamp-Viret, P., Duchamp, A., Sicard, G., 1990a. Olfactory discrimination over a wide concentration range: comparison of receptor cell and bulb neuron abilities. Brain Res. 517, 256–262.
Duchamp-Viret, P., Duchamp, A., Vigouroux, M., 1990b. Temporal aspects of information processing in the first two stages of the frog olfactory system: influence of stimulus intensity. Chem. Senses 15, 349–365.
Ennis, M., Linster, C., Aroniadou-Anderjaska, V., Ciombor, K., Shipley, M.T., 1998. Glutamate and synaptic plasticity at mammalian primary olfactory synapses. Ann. N. Y. Acad. Sci. 855, 457–466.
Escanilla, O., Arrellanos, A., Karnow, A., Ennis, M., Linster, C., 2010. Noradrenergic modulation of behavioral odor detection and discrimination thresholds in the olfactory bulb. Eur. J. Neurosci. 32, 458–468.
Escanilla, O., Alperin, S., Youssef, M., Ennis, M., Linster, C., 2012. Noradrenergic but not cholinergic modulation of olfactory bulb during processing of near threshold concentration stimuli. Behav. Neurosci. 126, 720–728.

Fantana, A.L., Soucy, E.R., Meister, M., 2008. Rat olfactory bulb mitral cells receive sparse glomerular inputs. Neuron 59, 802–814.

Firestein, S., Shepherd, G.M., 1991. A kinetic model of the odor response in single olfactory receptor neurons. J. Steroid Biochem. Mol. Biol. 39, 615–620.

Firestein, S., Picco, C., Menini, A., 1993. The relation between stimulus and response in olfactory receptor cells of the tiger salamander. J. Physiol. (Cambridge) 468, 1–10.

Fletcher, M.L., Masurkar, A.V., Xing, J., Imamura, F., Xiong, W., Nagayama, S., Mutoh, H., Greer, C.A., Knopfel, T., Chen, W.R., 2009. Optical imaging of postsynaptic odor representation in the glomerular layer of the mouse olfactory bulb. J. Neurophysiol. 102, 817–830.

Friedrich, R.W., Korsching, S.I., 1997. Combinatorial and chemotopic odorant coding in the zebrafish olfactory bulb visualized by optical imaging. Neuron 18, 737–752.

Gao, Y., Strowbridge, B.W., 2009. Long-term plasticity of excitatory inputs to granule cells in the rat olfactory bulb. Nat. Neurosci. 12, 731–733.

Geisler, W.S., 2008. Visual perception and the statistical properties of natural scenes. Annu. Rev. Psychol. 59, 167–192.

Getchell, T.V., 1986. Functional properties of vertebrate olfactory receptor neurons. Physiol. Rev. 66, 772–818.

Getchell, T.V., Shepherd, G.M., 1978. Responses of olfactory receptor cells to step pulses of odour at different concentrations in the salamander. J. Physiol. 282, 521–540.

Gire, D.H., Schoppa, N.E., 2009. Control of on/off glomerular signaling by a local GABAergic microcircuit in the olfactory bulb. J. Neurosci. 29, 13454–13464.

Guerin, D., Peace, S.T., Didier, A., Linster, C., Cleland, T.A., 2008. Noradrenergic neuromodulation in the olfactory bulb modulates odor habituation and spontaneous discrimination. Behav. Neurosci. 122, 816–826.

Haddad, R., Weiss, T., Khan, R., Nadler, B., Mandairon, N., Bensafi, M., Schneidman, E., Sobel, N., 2010. Global features of neural activity in the olfactory system form a parallel code that predicts olfactory behavior and perception. J. Neurosci. 30, 9017–9026.

Harrison, T.A., Scott, J.W., 1986. Olfactory bulb responses to odor stimulation: analysis of response pattern and intensity relationships. J. Neurophysiol. 56, 1571–1589.

Hasselmo, M.E., Anderson, B.P., Bower, J.M., 1992. Cholinergic modulation of cortical associative memory function. J. Neurophysiol. 67, 1230–1246.

Hayar, A., Shipley, M.T., Ennis, M., 2005. Olfactory bulb external tufted cells are synchronized by multiple intraglomerular mechanisms. J. Neurosci. 25, 8197–8208.

Imam, N., Cleland, T.A., Manohar, R., Merolla, P.A., Arthur, J.V., Akopyan, F., Modha, D.S., 2012. Implementation of olfactory bulb glomerular-layer computations in a digital neurosynaptic core. Front. Neurosci. 6, 83.

Johnson, B.A., Leon, M., 2007. Chemotopic odorant coding in a mammalian olfactory system. J. Comp. Neurol. 503, 1–34.

Johnson, B.A., Xu, Z., Ali, S.S., Leon, M., 2009. Spatial representations of odorants in olfactory bulbs of rats and mice: similarities and differences in chemotopic organization. J. Comp. Neurol. 514, 658–673.

Kay, L.M., Beshel, J., Brea, J., Martin, C., Rojas-Libano, D., Kopell, N., 2009. Olfactory oscillations: the what, how and what for. Trends Neurosci. 32, 207–214.

Kim, D.H., Phillips, M.E., Chang, A.Y., Patel, H.K., Nguyen, K.T., Willhite, D.C., 2011. Lateral connectivity in the olfactory bulb is sparse and segregated. Front. Neural Circuits 5, 5.

Kiyokage, E., Pan, Y.Z., Shao, Z., Kobayashi, K., Szabo, G., Yanagawa, Y., Obata, K., Okano, H., Toida, K., Puche, A.C., Shipley, M.T., 2010. Molecular identity of periglomerular and short axon cells. J. Neurosci. 30, 1185–1196.

Kohonen, T., Hari, R., 1999. Where the abstract feature maps of the brain might come from. Trends Neurosci. 22, 135–139.

Koppl, C., Gleich, O., Manley, G.A., 1993. An auditory fovea in the barn owl cochlea. J. Comp. Physiol. A. 171, 695–704.

Koulakov, A.A., Kolterman, B.E., Enikolopov, A.G., Rinberg, D., 2011. In search of the structure of human olfactory space. Front. Syst. Neurosci. 5, 65.

Krell, T., Lacal, J., Busch, A., Silva-Jimenez, H., Guazzaroni, M.E., Ramos, J.L., 2010. Bacterial sensor kinases: diversity in the recognition of environmental signals. Annu. Rev. Microbiol. 64, 539–559.

Lepousez, G., Lledo, P.M., 2013. Odor discrimination requires proper olfactory fast oscillations in awake mice. Neuron 80, 1010–1024.

Lepousez, G., Valley, M.T., Lledo, P.M., 2013. The impact of adult neurogenesis on olfactory bulb circuits and computations. Annu. Rev. Physiol. 75, 339–363.

Li, G., Cleland, T.A., 2013. A two-layer biophysical model of cholinergic neuromodulation in olfactory bulb. J. Neurosci. 33, 3037–3058.

Linster, C., Cleland, T.A., 2010. Decorrelation of odor representations via spike timing-dependent plasticity. Front. Comput. Neurosci. 4, 157.

Linster, C., Sachse, S., Galizia, G., 2005. Computational modeling suggests that response properties rather than spatial position determine connectivity between olfactory glomeruli. J. Neurophysiol. 93, 3410–3417.

Linster, C., Nai, Q., Ennis, M., 2011. Nonlinear effects of noradrenergic modulation of olfactory bulb function in adult rodents. J. Neurophysiol. 105, 1432–1443.

Liu, S., Shipley, M.T., 2008. Multiple conductances cooperatively regulate spontaneous bursting in mouse olfactory bulb external tufted cells. J. Neurosci. 28, 1625–1639.

Liu, S., Plachez, C., Shao, Z., Puche, A., Shipley, M.T., 2013. Olfactory bulb short axon cell release of GABA and dopamine produces a temporally biphasic inhibition-excitation response in external tufted cells. J. Neurosci. 33, 2916–2926.

Mandairon, N., Ferretti, C.J., Stack, C.M., Rubin, D.B., Cleland, T.A., Linster, C., 2006. Cholinergic modulation in the olfactory bulb influences spontaneous olfactory discrimination in adult rats. Eur. J. Neurosci. 24, 3234–3244.

Manella, L.C., Alperin, S., Linster, C., 2013. Stressors impair odor recognition memory via an olfactory bulb-dependent noradrenergic mechanism. Front. Integr. Neurosci. 7, 97.

Marbach, F., Albeanu, D.F., 2011. Photostimulation of short axon cells reveals widespread inhibition in the mouse olfactory bulb. Soc. Neurosci. Abstr. 475, 19.

McGann, J.P., 2013. Presynaptic inhibition of olfactory sensory neurons: new mechanisms and potential functions. Chem. Senses 38, 459–474.

Meredith, M., 1986. Patterned response to odor in mammalian olfactory bulb: the influence of intensity. J. Neurophysiol. 56, 572–597.

Mombaerts, P., 1999. Molecular biology of odorant receptors in vertebrates. Annu. Rev. Neurosci. 22, 487–509.

Mombaerts, P., 2001. The human repertoire of odorant receptor genes and pseudogenes. Annu. Rev. Genomics Hum. Genet. 2, 493–510.

Mombaerts, P., 2004. Odorant receptor gene choice in olfactory sensory neurons: the one receptor-one neuron hypothesis revisited. Curr. Opin. Neurobiol. 14, 31–36.

Mombaerts, P., Wang, F., Dulac, C., Chao, S.K., Nemes, A., Mendelsohn, M., Edmondson, J., Axel, R., 1996. Visualizing an olfactory sensory map. Cell 87, 675–686.

Moreno, M.M., Linster, C., Escanilla, O., Sacquet, J., Didier, A., Mandairon, N., 2009. Olfactory perceptual learning requires adult neurogenesis. Proc. Natl. Acad. Sci. U. S. A. 106, 17980–17985.

Moreno, M.M., Bath, K., Kuczewski, N., Sacquet, J., Didier, A., Mandairon, N., 2012. Action of the noradrenergic system on adult-born cells is required for olfactory learning in mice. J. Neurosci. 32, 3748–3758.

Mori, K., Takahashi, Y.K., Igarashi, K.M., Yamaguchi, M., 2006. Maps of odorant molecular features in the mammalian olfactory bulb. Physiol. Rev. 86, 409–433.

Morrison, E.E., Costanzo, R.M., 1990. Morphology of the human olfactory epithelium. J. Comp. Neurol. 297, 1–13.

Morrison, E.E., Costanzo, R.M., 1992. Morphology of olfactory epithelium in humans and other vertebrates. Microsc. Res. Tech. 23, 49–61.

Olshausen, B.A., Field, D.J., 2004. Sparse coding of sensory inputs. Curr. Opin. Neurobiol. 14, 481–487.

Parsa, P., D'Souza, R.D., Vijayaraghavan, S., 2011. GABA-induced calcium transients in juxtaglomerular neurons of the mouse olfactory bulb. Soc. Neurosci. Abstr. 475, 15.

Penfield, W., Rasmussen, T., 1950. The Cerebral Cortex of Man: A Clinical Study of Localization of Function. MacMillan, New York.

Pressler, R.T., Inoue, T., Strowbridge, B.W., 2007. Muscarinic receptor activation modulates granule cell excitability and potentiates inhibition onto mitral cells in the rat olfactory bulb. J. Neurosci. 27, 10969–10981.

Rall, W., Shepherd, G.M., 1968. Theoretical reconstruction of field potentials and dendrodendritic synaptic interactions in olfactory bulb. J. Neurophysiol. 31, 884–915.

Ravel, N., Elaagouby, A., Gervais, R., 1994. Scopolamine injection into the olfactory bulb impairs short-term olfactory memory in rats. Behav. Neurosci. 108, 317–324.

Rospars, J.P., Lansky, P., Duchamp-Viret, P., Duchamp, A., 2000. Spiking frequency versus odorant concentration in olfactory receptor neurons. Biosystems 58, 133–141.

Rubin, D.B., Cleland, T.A., 2006. Dynamical mechanisms of odor processing in olfactory bulb mitral cells. J. Neurophysiol. 96, 555–568.

Sahay, A., Wilson, D.A., Hen, R., 2011. Pattern separation: a common function for new neurons in hippocampus and olfactory bulb. Neuron 70, 582–588.

Schoenfeld, T.A., Cleland, T.A., 2005. The anatomical logic of smell. Trends Neurosci. 28, 620–627.

Sethupathy, P., Rubin, D.B., Li, G., Cleland, T.A., 2013. A model of electrophysiological heterogeneity in periglomerular cells. Front. Comput. Neurosci. 7, 49.

Shao, Z., Puche, A.C., Kiyokage, E., Szabo, G., Shipley, M.T., 2009. Two GABAergic intraglomerular circuits differentially regulate tonic and phasic presynaptic inhibition of olfactory nerve terminals. J. Neurophysiol. 101, 1988–2001.

Shao, Z., Puche, A.C., Shipley, M.T., 2013. Intraglomerular inhibition maintains mitral cell response contrast across input frequencies. J. Neurophysiol. 110, 2185–2191.

Soucy, E.R., Albeanu, D.F., Fantana, A.L., Murthy, V.N., Meister, M., 2009. Precision and diversity in an odor map on the olfactory bulb. Nat. Neurosci. 12, 210–220.

Strotmann, J., Breer, H., 2006. Formation of glomerular maps in the olfactory system. Semin. Cell Dev. Biol. 17, 402–410.

Suga, N., Zhang, Y., Yan, J., 1997. Sharpening of frequency tuning by inhibition in the thalamic auditory nucleus of the mustached bat. J. Neurophysiol. 77, 2098–2114.

Timme, M., Geisel, T., Wolf, F., 2006. Speed of synchronization in complex networks of neural oscillators: analytic results based on Random Matrix Theory. Chaos 16, 015108.
Trotier, D., 1994. Intensity coding in olfactory receptor cells. Semin. Cell Biol. 5, 47–54.
Wachowiak, M., Cohen, L.B., Zochowski, M.R., 2002. Distributed and concentration-invariant spatial representations of odorants by receptor neuron input to the turtle olfactory bulb. J. Neurophysiol. 87, 1035–1045.
Wellis, D.P., Scott, J.W., Harrison, T.A., 1989. Discrimination among odorants by single neurons of the rat olfactory bulb. J. Neurophysiol. 61, 1161–1177.
Willhite, D.C., Nguyen, K.T., Masurkar, A.V., Greer, C.A., Shepherd, G.M., Chen, W.R., 2006. Viral tracing identifies distributed columnar organization in the olfactory bulb. Proc. Natl. Acad. Sci. U. S. A. 103, 12592–12597.
Wilson, D.A., 2009. Pattern separation and completion in olfaction. Ann. N. Y. Acad. Sci. 1170, 306–312.
Yang, L., Pollak, G.D., Resler, C., 1992. GABAergic circuits sharpen tuning curves and modify response properties in the mustache bat inferior colliculus. J. Neurophysiol. 68, 1760–1774.
Yokoi, M., Mori, K., Nakanishi, S., 1995. Refinement of odor molecule tuning by dendrodendritic synaptic inhibition in the olfactory bulb. Proc. Natl. Acad. Sci. U. S. A. 92, 3371–3375.
Zaidi, Q., Victor, J., McDermott, J., Geffen, M., Bensmaia, S., Cleland, T.A., 2013. Perceptual spaces: mathematical structures to neural mechanisms. J. Neurosci. 33, 17597–17602.
Zook, J.M., Leake, P.A., 1989. Connections and frequency representation in the auditory brainstem of the mustache bat, Pteronotus parnellii. J. Comp. Neurol. 290, 243–261.
Zufall, F., Leinders-Zufall, T., 2000. The cellular and molecular basis of odor adaptation. Chem. Senses 25, 473–481.

Progress in Brain Research
Volume 208

# Odor Memory and Perception

Edited by

**Edi Barkai**
*Sagol Department of Neurobiology, University of Haifa*
*Haifa, Israel*

**Donald A. Wilson**
*Emotional Brain Institute, Nathan Kline Institute*
*for Psychiatric Research, and*
*Department of Child and Adolescent Psychiatry, New York*
*University Langone School of Medicine*
*New York, USA*

ELSEVIER
AMSTERDAM • BOSTON • HEIDELBERG • LONDON • NEW YORK • OXFORD
PARIS • SAN DIEGO • SAN FRANCISCO • SINGAPORE • SYDNEY • TOKYO